

Preparation of Textured $\text{Bi}_{0.5}(\text{Na,K})_{0.5}\text{TiO}_3\text{-BiFeO}_3$ Solid Solutions by Reactive-Templated Grain Growth Process

Kyoko Kato and Toshio Kimura[†]

*School of Integrated Design Engineering, Graduate School of Science and Technology,
Keio University, Yokohama 223-8522, Japan*

(Received October 19, 2006; Accepted October 27, 2006)

ABSTRACT

Textured $\text{Bi}_{0.5}(\text{Na,K})_{0.5}\text{TiO}_3\text{-BiFeO}_3$ ceramics were prepared by the reactive-templated grain growth process, using platelike $\text{Bi}_4\text{Ti}_3\text{O}_{12}$ particles. The effects of chemical composition in $\text{Bi}_{0.5}(\text{Na,K})_{0.5}\text{TiO}_3$ on texture development and densification were examined. Textured ceramics were obtained by using $\text{Bi}_{0.5}\text{K}_{0.5}\text{TiO}_3$ as an end member of the solid solution but densification was limited. Dense ceramics were obtained by using $\text{Bi}_{0.5}\text{Na}_{0.5}\text{TiO}_3$ but texture did not develop. Dense, textured ceramics were obtained by using $\text{Bi}_{0.5}(\text{Na}_{0.5}\text{K}_{0.5})_{0.5}\text{TiO}_3$.

Key words : *Texture, Reactive-templated grain growth, Solid solutions, $\text{Bi}_{0.5}\text{Na}_{0.5}\text{TiO}_3$, $\text{Bi}_{0.5}\text{K}_{0.5}\text{TiO}_3$, BiFeO_3*

1. Introduction

The methods to enhance the physical properties of ceramics contain (1) the search of new materials, (2) the selection of additives and (3) the optimization of microstructure. The development of texture is a technique belonging to category (3), and significant enhancement in piezoelectric properties is reported.¹⁾ Typical methods to develop texture in piezoelectric ceramics are (1) to form green compacts using anisometric particles,²⁻⁵⁾ (2) to apply pressure during heating,^{6,7)} and (3) to apply a magnetic field during consolidation of colloidal particles.⁸⁾ These techniques are applicable to compounds with large anisotropy in crystal structure. The development of texture in compounds with the perovskite structure is important, because typical piezoelectric ceramics have this structure, but the technique is limited. Only exception is the Reactive-Templated Grain Growth (RTGG) method.

In the RTGG process,⁵⁾ a precursor of a target compound (for example, $\text{Bi}_{0.5}\text{Na}_{0.5}\text{TiO}_3$) is selected: it should have an anisometric shape (e.g., platelike $\text{Bi}_4\text{Ti}_3\text{O}_{12}$). A complementary compound(s) (e.g., Na_2CO_3 and TiO_2) for the target compound is mixed. The mixture is tape-cast to form thin sheets in which the anisometric particles are aligned. A green compact is made by stacking the cast sheets, and then calcined. The target compound is formed by calcination. Two kinds of grains are formed in the calcined compact; aligned grains, which are transformed from the anisometric precursor particles, and randomly oriented grains. They are called tem-

plate and matrix grains, respectively. Sintering causes the growth of template grains at the expense of matrix grains, resulting in the development of texture. Thus, textured ceramics with the perovskite structure are prepared by using anisometric precursor particles.

The RTGG method has two advantages: this method can develop texture in compounds with an isotropic crystal structure, as mentioned above, and can be applicable to solid solutions with complex compositions, as exemplified for the systems $\text{Bi}_{0.5}(\text{Na,K})_{0.5}\text{TiO}_3$,⁹⁾ $\text{Bi}_{0.5}(\text{Na,K})_{0.5}\text{TiO}_3\text{-PbTiO}_3$,¹⁰⁾ and $\text{Bi}_{0.5}(\text{Na,K})_{0.5}\text{TiO}_3\text{-BaTiO}_3$.¹¹⁾ These are solid solutions with A-site substitution. Recently, good candidates for lead-free piezoelectric ceramics have been reported; they are $(\text{K,Na,Li})(\text{Nb,Ta,Sb})\text{O}_3$, solid solutions with A- and B-site substitutions.¹²⁾ It is expected that the material transport through the B-sites of perovskite is more difficult than that through the A-sites from a crystal structural point of view: An oxygen ion locates between neighboring B-sites and may hinder diffusion through B-sites, but no ion is present between neighboring A-sites. Therefore, it is important to find factors determining texture development in B-site-substituted materials.

This paper deals with the effect of an end member composition on texture development in $\text{Bi}_{0.5}(\text{Na,K})_{0.5}\text{TiO}_3\text{-BiFeO}_3$ solid solutions. The reasons for selecting these solid solutions are that $\text{Bi}_{0.5}(\text{Na,K})_{0.5}\text{TiO}_3$ is easily textured by the RTGG process using platelike $\text{Bi}_4\text{Ti}_3\text{O}_{12}$ (BiT) particles as reactive templates,⁵⁾ and that BiFeO_3 is one of the simplest perovskite compounds with Bi as A-site cations.¹³⁾

2. Experimental Procedure

Chemically pure Bi_2O_3 , TiO_2 , Na_2CO_3 , K_2CO_3 , and Fe_2O_3

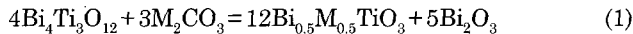
[†]Corresponding author : Toshio Kimura

E-mail : kimura@applc.keio.ac.jp

Tel : +81-45-566-1565 Fax : +81-45-566-1551

were used as raw materials. Platelike BiT particles were prepared from Bi_2O_3 and TiO_2 by molten salt synthesis at 1100°C for 1 h, using a NaCl-KCl mixture (1:1 molar ratio).¹⁴ The product was washed with deionized water several times to remove residual NaCl and KCl. The obtained BiT particles had a platelike shape, with an average diameter of about $10\ \mu\text{m}$ and thickness of $0.3\ \mu\text{m}$.

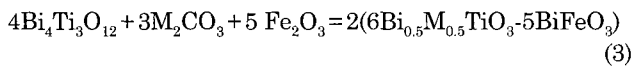
The composition of solid solutions was determined by the following considerations. Template $\text{Bi}_{0.5}(\text{Na},\text{K})_{0.5}\text{TiO}_3$ grains are formed by the reaction of platelike BiT particles with M_2CO_3 ($\text{M}=\text{Na}, \text{K}$).¹⁾



Bi_2O_3 formed by reaction (1) reacts with Fe_2O_3 to form BiFeO_3 .



Finally, $\text{Bi}_{0.5}\text{M}_{0.5}\text{TiO}_3$ and BiFeO_3 form homogeneous solid solution, $\text{Bi}_{0.5}\text{M}_{0.5}\text{TiO}_3\text{-BiFeO}_3$. The total reaction is expressed by reaction (3), which indicates the composition of the solid solution ($6\text{Bi}_{0.5}\text{M}_{0.5}\text{TiO}_3\text{-5BiFeO}_3$).



The solid solutions with three compositions were prepared in the present work; they were $6\text{Bi}_{0.5}\text{K}_{0.5}\text{TiO}_3\text{-5BiFeO}_3$, $6\text{Bi}_{0.5}\text{Na}_{0.5}\text{TiO}_3\text{-5BiFeO}_3$, and $6\text{Bi}_{0.5}(\text{Na}_{0.5}\text{K}_{0.5})_{0.5}\text{TiO}_3\text{-5BiFeO}_3$. The platelike BiT particles were mixed with Na_2CO_3 , K_2CO_3 , Fe_2O_3 , binder (poly(vinyl butyral)), plasticizer (di-*n*-butyl phthalate), and solvent (60 vol% toluene-40 vol% ethanol) in a planetary-ball mill for 2 h. The slurries were tape-cast to form a sheet, in which platelike BiT particles were aligned with their plate face parallel to the sheet surface. The sheets were cut, laminated, and pressed at a temperature of 80°C and pressure of 50 MPa for 3 min to form green compacts about 2 mm thick. The compacts were further cut into small pieces ($10 \times 10\ \text{mm}$).

The green compacts were heated at 700°C for 2 h in an ambient atmosphere to remove organic ingredients. Then, the compacts were isostatically pressed under a pressure of 98 MPa for 2 min at room temperature, and sintered at a temperature between 800° and 1100°C for 5 h.

The crystalline phases and the degree of orientation were determined by X-Ray Diffraction (XRD) analysis using $\text{CuK}\alpha$ radiation on the major surface of the sintered compacts. The degree of orientation was calculated using the following equations (the Lotgering method).¹⁵⁾

$$F = \frac{p-p_0}{1-p_0} \quad (4)$$

$$p = \frac{\sum I_{\{100\}}}{\sum I_{\{hkl\}}} \quad (5)$$

$$p_0 = \frac{\sum I_{0\{100\}}}{I_{0\{hkl\}}} \quad (6)$$

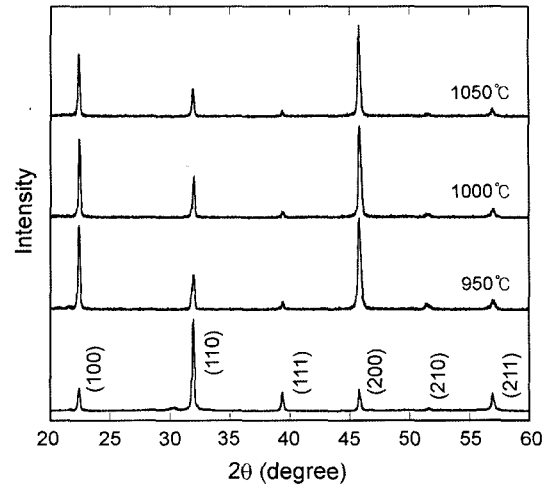


Fig. 1. XRD patterns of $\text{Bi}_{0.5}\text{K}_{0.5}\text{TiO}_3\text{-BiFeO}_3$ specimens sintered at indicated temperatures for 5 h. The pattern at the bottom is for powdered specimen sintered at 1000°C .

where I and I_0 are the peak heights for the sintered compacts and powdered specimen, respectively, and $\{100\}$ and $\{hkl\}$ are the Miller indexes. Diffraction lines in the 2θ range from 20° to 60° were used for the calculation.

The microstructure was observed with a Scanning Electron Microscopy (SEM) on the fractured, side surface of the sintered compacts. The distribution of elements was determined with an Electron-Probe Microanalyzer (EPMA). The theoretical densities were calculated from the lattice parameters determined by XRD. They were 7.039 , 7.111 , and $7.060\ \text{g/cm}^3$ for $6\text{Bi}_{0.5}\text{K}_{0.5}\text{TiO}_3\text{-5BiFeO}_3$, $6\text{Bi}_{0.5}\text{Na}_{0.5}\text{TiO}_3\text{-5BiFeO}_3$, and $6\text{Bi}_{0.5}(\text{Na}_{0.5}\text{K}_{0.5})_{0.5}\text{TiO}_3\text{-5BiFeO}_3$, respectively.

3. Results and Discussion

3.1. $\text{Bi}_{0.5}\text{K}_{0.5}\text{TiO}_3\text{-BiFeO}_3$ System

Fig. 1 shows the XRD patterns of $\text{Bi}_{0.5}\text{K}_{0.5}\text{TiO}_3\text{(BKT)-BiFeO}_3$ specimens sintered at various temperatures. The pattern shown at the bottom of Fig. 1 shows the diffraction pattern of the powdered specimen sintered at 1000°C . It was judged that the perovskite formation was almost finished at 950°C . The relative intensity for the specimens sintered between 950° and 1050°C was different from that of the powdered specimen; the sintered specimens had strong (100) and (200) peaks, indicating the evolution of $\langle 100 \rangle$ -texture. The F value was about 0.65 for three specimens.

Fig. 2 shows the microstructures of specimens heated at various temperatures. The relative density is indicated in the figure. The microstructures of specimens heated at 900° and 950°C were composed of platelike and equiaxed grains. These grains had the perovskite structure, as judged from the XRD patterns (Fig. 1). The platelike nature of grains was maintained up to 1050°C .

Figs. 3 and 4 show the distribution of Bi, Fe, Ti, and K ions in the specimens sintered at 900° and 1050°C , respec-

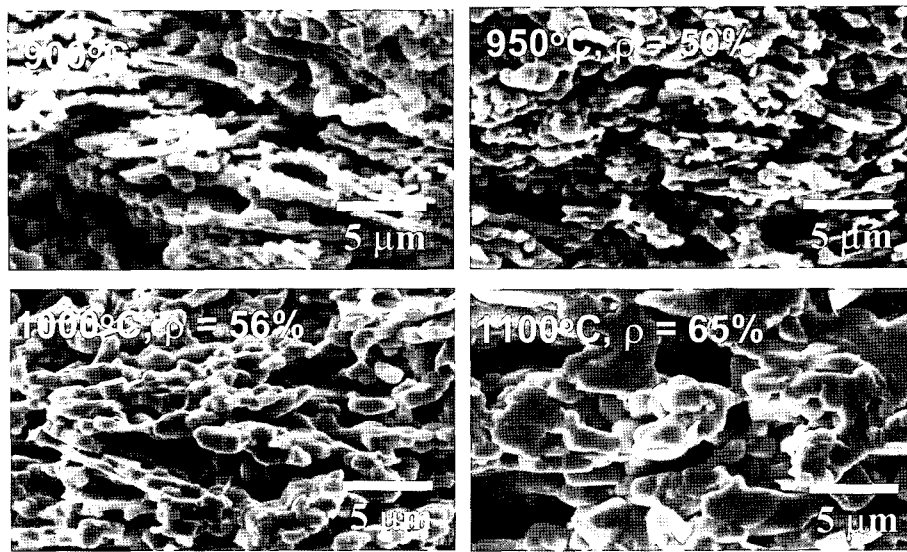


Fig. 2. Microstructures of $\text{Bi}_{0.5}\text{K}_{0.5}\text{TiO}_3\text{-BiFeO}_3$ specimens sintered at indicated temperatures for 5 h. The relative density (ρ) is also indicated.

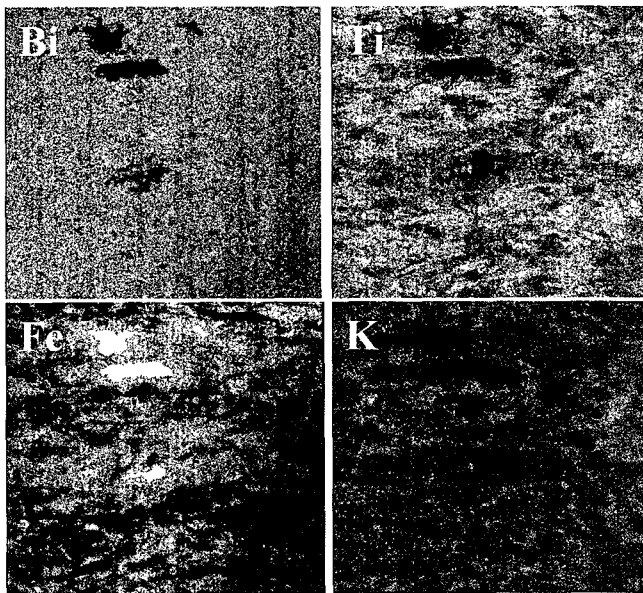


Fig. 3. Distribution of elements in $\text{Bi}_{0.5}\text{K}_{0.5}\text{TiO}_3\text{-BiFeO}_3$ specimen sintered at 900°C for 5 h.

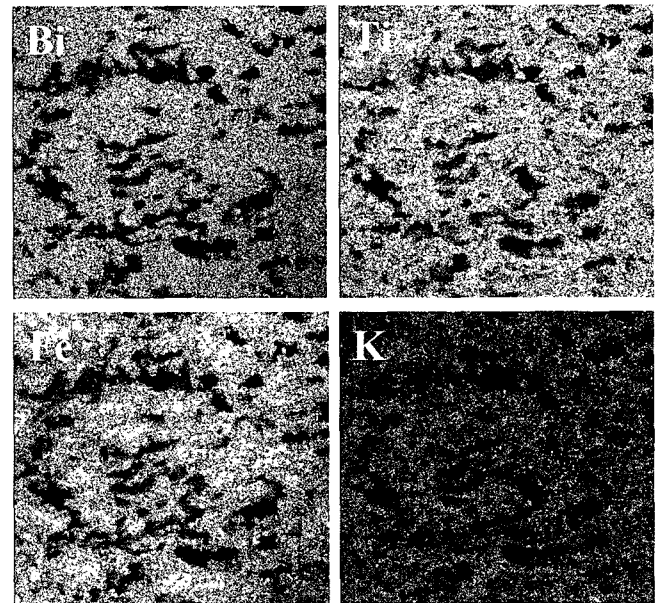


Fig. 4. Distribution of elements in $\text{Bi}_{0.5}\text{K}_{0.5}\text{TiO}_3\text{-BiFeO}_3$ specimen sintered at 1050°C for 5 h.

tively. For the specimen sintered at 900°C, a strong Fe signal indicated the presence of unreacted Fe_2O_3 . In other parts, the positions with high Fe concentration contained Bi ions but fewer amounts of Ti and K ions. On the contrary, the positions with high Ti concentration contained Bi and K but fewer amounts of Fe ions. This indicated the separate presence of BiFeO_3 and BKT grains. The distribution of ions was homogenized by heating at 1050°C (dark positions in the figure are pores), indicating the formation of $\text{Bi}_{0.5}\text{K}_{0.5}\text{TiO}_3\text{-BiFeO}_3$ solid solution.

Fig. 5 schematically shows the reaction sequence. The diffusion of K_2O into platelike BiT particle forms platelike

BKT grains by reaction (1). The orientation of a-axis of platelike BKT is determined by the orientation of c-axis of BiT,¹⁶⁾ which is perpendicular to the plate face, and platelike BKT acts as template for texture evolution. Bi_2O_3 formed by reaction (1) reacts with Fe_2O_3 to form BiFeO_3 by reaction (2). Because the reactants of this reaction have no specific orientation of crystal axes, the formed BiFeO_3 grains have random orientation. Thus, BKT with specific orientation and BiFeO_3 with random orientation are formed at different positions. Heating at high temperatures causes solid solution formation. The evolution of texture and the presence of platelike grains at 1050°C indicate that BiFeO_3

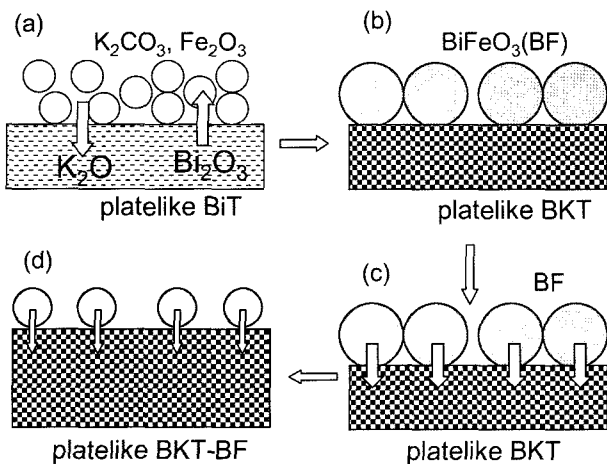


Fig. 5. Schematic diagram of reaction of BiT with K_2CO_3 and Fe_2O_3 .

diffuses into BKT grains during the solid solution formation. The resultant solid solution grains have the same orientation as BKT.

The textured $Bi_{0.5}K_{0.5}TiO_3$ - $BiFeO_3$ solid solution was obtained by the RTGG process, but a problem was its low density (the density value is shown in Fig. 2). So, the formation of $Bi_{0.5}Na_{0.5}TiO_3$ - $BiFeO_3$ solid solution was examined.

3.2. $Bi_{0.5}Na_{0.5}TiO_3$ - $BiFeO_3$ System

Fig. 6 shows the XRD patterns of $Bi_{0.5}Na_{0.5}TiO_3$ (BNT)- $BiFeO_3$ specimens sintered at various temperatures. The perovskite formation was almost finished at 800°C. The relative intensity of diffraction lines was not dependent on the heating temperature and was almost the same as that of

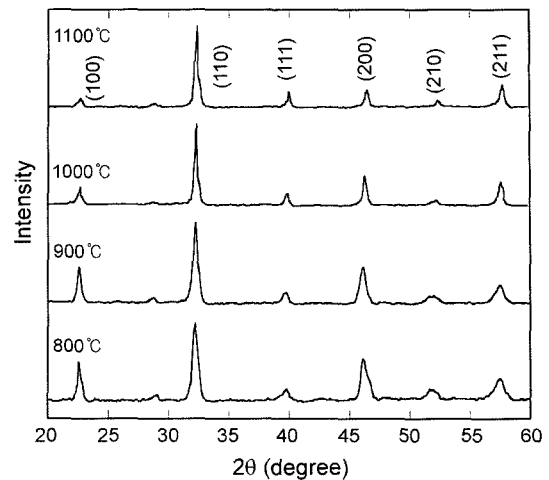


Fig. 6. XRD patterns of $Bi_{0.5}Na_{0.5}TiO_3$ - $BiFeO_3$ specimens sintered at indicated temperatures for 5 h.

non-textured specimen. This result indicated that texture did not develop in these specimens.

Fig. 7 shows the microstructures of specimens heated at various temperatures. The relative density is indicated in the figure. The microstructures of specimens heated at 800°C and 900°C were composed of platelike and equiaxed grains. These grains had the perovskite structure, as indicated by the XRD patterns (Fig. 6). The platelike grains changed to be equiaxed by heating at and above 1000°C.

The distribution of Bi, Fe, Ti, and Na ions in the specimens sintered at 800°C had the same characteristics as those shown in Fig. 3; some parts contained Fe and Bi ions and the other parts contained Bi, Na, and Ti ions, indicating the formation of $BiFeO_3$ and $Bi_{0.5}Na_{0.5}TiO_3$ at different posi-

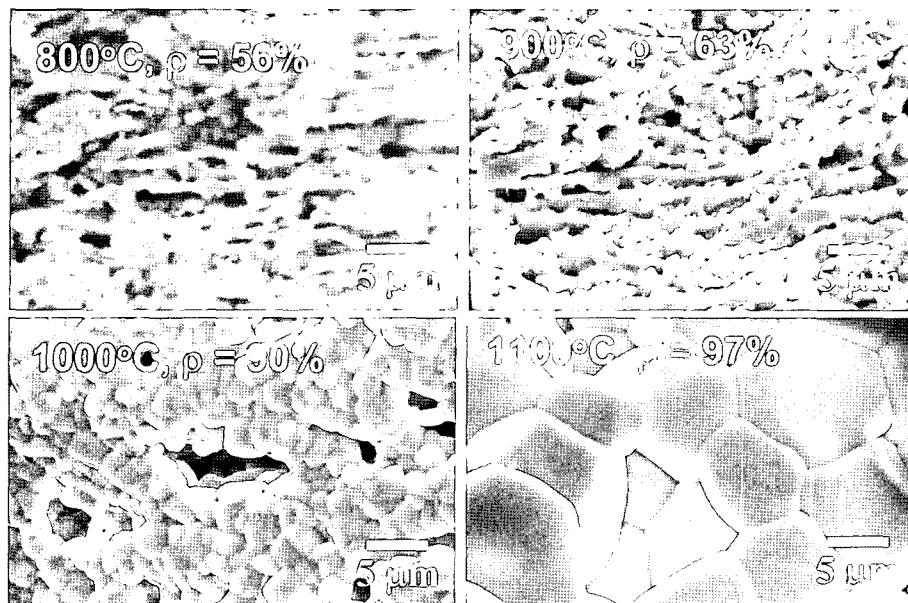


Fig. 7. Microstructures of $Bi_{0.5}Na_{0.5}TiO_3$ - $BiFeO_3$ specimens sintered at indicated temperatures for 5 h. The relative density (ρ) is also indicated.

tions. The homogeneous distribution of all cations was observed in the specimen sintered at 1000°C , indicating the formation of $\text{Bi}_{0.5}\text{Na}_{0.5}\text{TiO}_3\text{-BiFeO}_3$ solid solution.

These results indicate that the reaction mechanisms of the formation of the $\text{Bi}_{0.5}\text{Na}_{0.5}\text{TiO}_3\text{-BiFeO}_3$ solid solution are the same as those of the $\text{Bi}_{0.5}\text{K}_{0.5}\text{TiO}_3\text{-BiFeO}_3$ solid solution schematically shown in Fig. 5, except for the direction of material transport during solid solution formation. $\text{Bi}_{0.5}\text{Na}_{0.5}\text{TiO}_3$ diffuses into BiFeO_3 grains, resulting in the disappearance of platelike grains which are necessary to evolve texture.

The comparison between Figs. 2 and 7 indicates that the use of $\text{Bi}_{0.5}\text{Na}_{0.5}\text{TiO}_3$ instead of $\text{Bi}_{0.5}\text{K}_{0.5}\text{TiO}_3$ as an end member of solid solution is beneficial to obtain dense materials. This might be caused by the difference in diffusivity between Na and K ions. The ionic radii of A site cations are Bi:0.117 nm, Na:0.116 nm, and K:0.152 nm (the coordination number is 6).¹⁷ It is expected that the diffusivity of large K ions is smaller than that of other cations. Therefore, the perovskite phases were formed at lower temperatures in the $\text{Bi}_{0.5}\text{Na}_{0.5}\text{TiO}_3\text{-BiFeO}_3$ system (at 800°C) than $\text{Bi}_{0.5}\text{K}_{0.5}\text{TiO}_3\text{-BiFeO}_3$ (at 950°C). Larger diffusivity of Na ions than K ions increases the densification rate but causes the material transport from $\text{Bi}_{0.5}\text{Na}_{0.5}\text{TiO}_3$ to BiFeO_3 during the solid solution formation. This hinders texture development. So, the use of $\text{Bi}_{0.5}(\text{Na}_{0.5}\text{K}_{0.5})_{0.5}\text{TiO}_3$ as an end member of solid solution was examined.

3.3. $\text{Bi}_{0.5}(\text{Na}_{0.5}\text{K}_{0.5})_{0.5}\text{TiO}_3\text{-BiFeO}_3$ System

Fig. 8 shows the XRD patterns of the $\text{Bi}_{0.5}(\text{Na}_{0.5}\text{K}_{0.5})_{0.5}\text{TiO}_3(\text{BNKT})\text{-BiFeO}_3$ specimens sintered at various temperatures. The comparison of the pattern with that of powdered specimen indicates the evolution of $\langle 100 \rangle$ -texture. The degree of orientation was increased by increasing temperature (0.43 at 900°C , 0.49 at 1000°C and 0.72 at 1100°C).

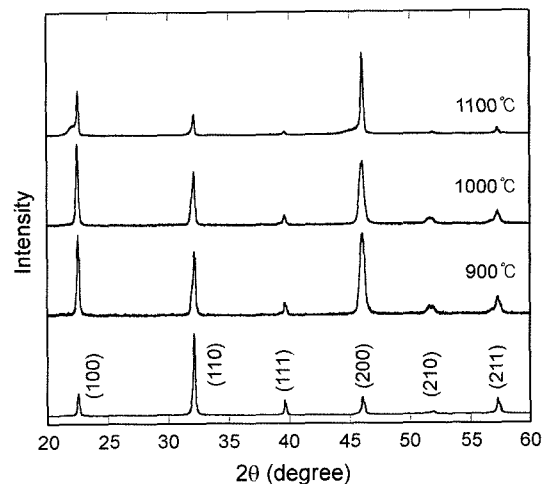


Fig. 8. XRD patterns of $\text{Bi}_{0.5}(\text{Na}_{0.5}\text{K}_{0.5})_{0.5}\text{TiO}_3\text{-BiFeO}_3$ specimens sintered at indicated temperatures for 5 h. The pattern at the bottom is for powdered specimen sintered at 1000°C .

Fig. 9 shows the microstructures of the compacts, together with the density, which indicates that the dense ceramics were obtained by using BNKT as an end member of solid solution. The platelike nature of grains remained up to 1000°C , and these grains increased their thickness, indicating the growth of platelike grains at the expense of equiaxed, randomly oriented grains.

These results indicate that dense, highly-textured ceramics with the B-site substituted perovskite structure were obtained by using BNKT as an end member of the solid solution. The presence of K ions prevents the disappearance of platelike grains, which act as templates for texture development, by small diffusivity to maintain the direction of diffusion from BiFeO_3 to BNKT grains during solid solution

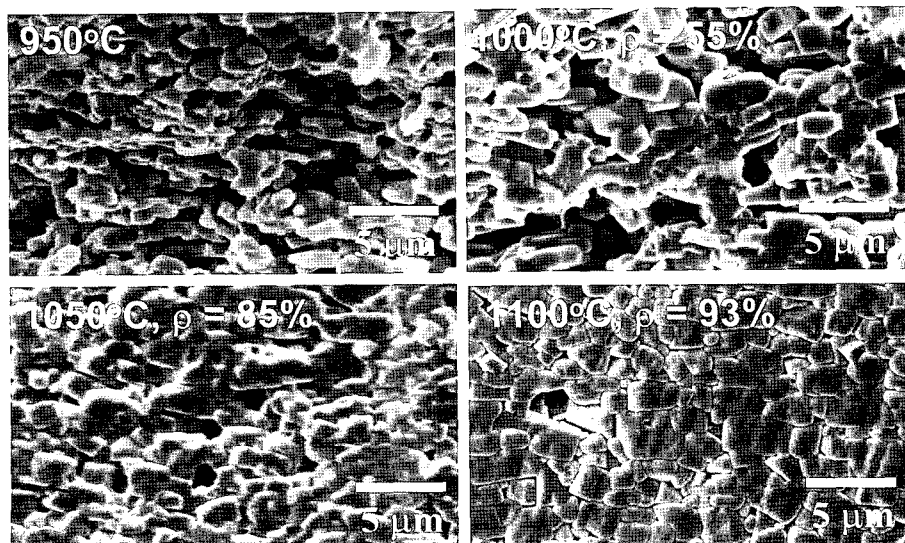


Fig. 9. Microstructures of $\text{Bi}_{0.5}(\text{Na}_{0.5}\text{K}_{0.5})_{0.5}\text{TiO}_3\text{-BiFeO}_3$ specimens sintered at indicated temperatures for 5 h. The relative density (ρ) is also indicated.

formation. The partial substitution of Na ions for K ions increases the diffusivity of A-site cations to promote densification.

3.4. Control of Composition

So far, the solid solutions with the composition $6\text{Bi}_{0.5}(\text{Na,K})_{0.5}\text{TiO}_3\text{-}5\text{BiFeO}_3$ have been dealt with. This composition was determined by equation (3), in which Bi_2O_3 to form BiFeO_3 is supplied from platelike $\text{Bi}_4\text{Ti}_3\text{O}_{12}$ by reaction (1). One of the merits of the RTGG process is its applicability to solid solutions with various compositions. Therefore, the present process was applied to the solid solutions with the compositions different from $6\text{Bi}_{0.5}(\text{Na,K})_{0.5}\text{TiO}_3\text{-}5\text{BiFeO}_3$. They were $3\text{Bi}_{0.5}(\text{Na}_{0.5}\text{K}_{0.5})_{0.5}\text{TiO}_3\text{-}3\text{BiFeO}_3$ (3BNKT-BF) and $\text{Bi}_{0.5}(\text{Na}_{0.5}\text{K}_{0.5})_{0.5}\text{TiO}_3\text{-}3\text{BiFeO}_3$ (BNKT-3BF).

The starting mixtures were prepared by adding the raw materials to the mixture containing platelike $\text{Bi}_4\text{Ti}_3\text{O}_{12}$, Na_2CO_3 , K_2CO_3 , and Fe_2O_3 . For 3BNKT-BF, $(4.5\text{Bi}_2\text{O}_3 + 2.25\text{Na}_2\text{CO}_3 + 2.25\text{K}_2\text{CO}_3 + 18\text{TiO}_2)$ were added to $(4\text{Bi}_4\text{Ti}_3\text{O}_{12} + 1.5\text{Na}_2\text{CO}_3 + 1.5\text{K}_2\text{CO}_3 + 5\text{Fe}_2\text{O}_3)$, and for BNKT-3BF, $(13\text{Bi}_2\text{O}_3 + 13\text{Fe}_2\text{O}_3)$ were added to $(4\text{Bi}_4\text{Ti}_3\text{O}_{12} + 1.5\text{Na}_2\text{CO}_3 + 1.5\text{K}_2\text{CO}_3 + 5\text{Fe}_2\text{O}_3)$. The sintered compacts were prepared by the same procedure used for $6\text{Bi}_{0.5}(\text{Na}_{0.5}\text{K}_{0.5})_{0.5}\text{TiO}_3\text{-}5\text{BiFeO}_3$ (6BNKT-5BF). The 3BNKT-BF specimen had the density

more than 90% of the theoretical value at 1100°C and the BNNKT-3BF at 900°C by heating for 5 h.

Fig. 10 shows the degree of orientation of 3BNKT-BF and BNKT-3BF, together with 6BNKT-5BF, as a function of sintering temperature, and Fig. 11 shows the microstructures of sintered compacts. 3BNKT-BF had a smaller F value than 6BNKT-5BF at 900° and 950°C because of the presence of randomly oriented BNKT formed from $(4.5\text{Bi}_2\text{O}_3 + 2.25\text{Na}_2\text{CO}_3 + 2.25\text{K}_2\text{CO}_3 + 18\text{TiO}_2)$, but the F value of 3BNKT-BF reached almost the same value as that of 6BNKT-5BF at 1000°C . The microstructure of 3BNKT-BF at 1100°C was composed of platelike grains. Probably, randomly oriented BNKT diffuses into template grains to form the solid solution with the composition of 3BNKT-BF. Therefore, the textured ceramics with a similar F value to that of 6BNKT-5BF were obtained. An increase in the BNKT concentration enhances the formation of grains with a platelike character (compare Fig. 9 to Fig. 11), because cubic grains develop in sintered $\text{Bi}_{0.5}(\text{Na}_{0.5}\text{K}_{0.5})_{0.5}\text{TiO}_3$.¹⁸⁾

The F value of BNKT-3BF was small (Fig. 10), and the sintered compact was composed of equiaxed grains (Fig. 11). This result suggests that an increase in the BiFeO_3 concentration hinders the diffusion from BiFeO_3 to BNKT grains. Rather, the diffusion from templated BNKT grains to randomly oriented BiFeO_3 grains might be dominant. Probably, the diffusivity of BNKT and BiFeO_3 is different and a dominant direction of diffusion is determined by the relative amount of each phase.

4. Conclusions

Textured $\text{Bi}_{0.5}(\text{Na,K})_{0.5}\text{TiO}_3\text{-}3\text{BiFeO}_3$ solid solutions were prepared by the RTGG process to examine the factors controlling texture development in B-site substituted perovskite phase. The degree of orientation and the sintered density were dependent on the chemical composition of $\text{Bi}_{0.5}(\text{Na,K})_{0.5}\text{TiO}_3$ phase and the overall composition of solid solution. $\text{Bi}_{0.5}\text{K}_{0.5}\text{TiO}_3$ gave textured solid solution but densification was limited. $\text{Bi}_{0.5}\text{Na}_{0.5}\text{TiO}_3$ gave dense solid solution but texture did not develop. $\text{Bi}_{0.5}(\text{Na}_{0.5}\text{K}_{0.5})_{0.5}\text{TiO}_3$ gave dense, textured solid solution. An increase in the BiFeO_3 concentration hindered the development of texture. At first, it is expected that the cations in the B-sites determine the evolution of texture, but it is realized that the diffusivity of

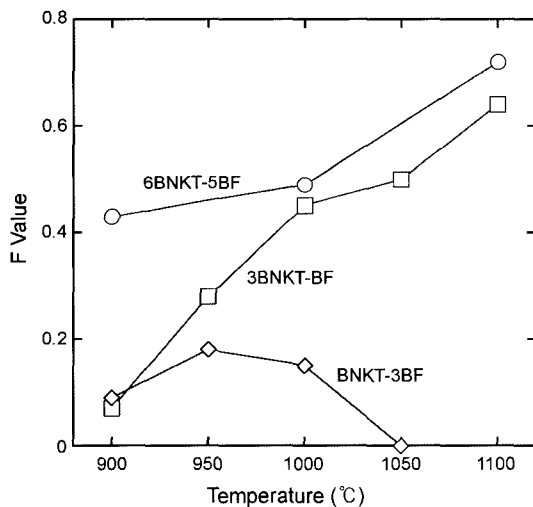


Fig. 10. Effect of solid solution composition on texture development.

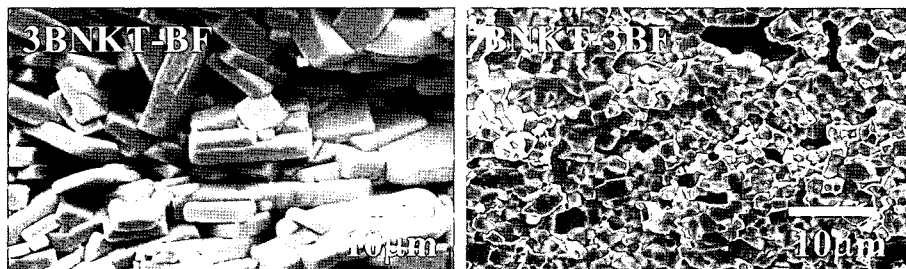


Fig. 11. Microstructures of 3BNKT-BF and BNKT-3BF specimens sintered at 1100° and 900°C , respectively, for 5 h.

A-site cations is also important and the slowest cations determine the direction of material transport during solid solution formation. The volume ratio of template and matrix grains also important to prevent the disappearance of template grains.

REFERENCES

1. T. Kimura, "Application of Texture Engineering to Piezoelectric Ceramics -A Review-," *J. Ceram. Soc. Jpn.*, **114** [1] 15-25 (2006).
2. M. Granahan, M. Holmes, W. A. Schulze, and R. E. Newnham, "Grain-Oriented PbNb_2O_6 Ceramics," *J. Am. Ceram. Soc.*, **64** [4] C-68-C-69 (1981).
3. S. Swartz, W. A. Schulze, and J. V. Biggers, "Fabrication and Electrical Properties of Grain Oriented $\text{Bi}_4\text{Ti}_3\text{O}_{12}$ Ceramics," *Ferroelectrics*, **38** [1-4] 765-68 (1981).
4. J. A. Horn, S. C. Zhang, U. Selvaraj, G. L. Messing, and S. Trolier-McKinstry, "Templated Grain Growth of Textured Bismuth Titanate," *J. Am. Ceram. Soc.*, **82** [4] 921-26 (1999).
5. T. Tani, "Crystalline-Oriented Piezoelectric Bulk Ceramics with a Perovskite-Type Structure," *J. Kor. Phys. Soc.*, **32** S1217-20 (1998).
6. H. Igarashi, K. Matsunaga, T. Taniai, and K. Okazaki, "Dielectric and Piezoelectric Properties of Grain-Oriented $\text{PbBi}_2\text{Nb}_2\text{O}_9$ Ceramics," *Am. Ceram. Soc. Bull.*, **57** [9] 815-17 (1978).
7. T. Takenaka and K. Sakata, "Grain Orientation and Electrical Properties of Hot-Forged $\text{Bi}_4\text{Ti}_3\text{O}_{12}$ Ceramics," *Jpn. J. Appl. Phys.*, **19** [1] 31-9 (1980).
8. A. Makiya, D. Kusano, S. Tanaka, N. Uchida, K. Uematsu, T. Kimura, K. Kitazawa, and Y. Doshida, "Particle Oriented Bismuth Titanate Ceramics Made in High Magnetic Field," *J. Ceram. Soc. Jpn.*, **111** [9] 702-04 (2003).
9. E. Fukuchi, T. Kimura, T. Tani, T. Takeuchi, and Y. Saito, "Effect of Potassium Concentration on the Grain Orientation in Bismuth Sodium Potassium Titanate," *J. Am. Ceram. Soc.*, **85** [6] 1461-66 (2002).
10. Y. Abe and T. Kimura, "Factors Determining Grain Orientation in Bismuth Sodium Potassium Titanate-Lead Zirconate Titanate Solid Solutions Made by Reactive Templated Grain Growth Method," *J. Am. Ceram. Soc.*, **85** [5] 1114-20 (2002).
11. T. Kimura, T. Takahashi, T. Tani, and Y. Saito, "Preparation of Crystallographically Textured $\text{Bi}_{0.5}\text{Na}_{0.5}\text{TiO}_3\text{-BaTiO}_3$ Ceramics by Reactive-Templated Grain Growth Method," *Ceram. International*, **30** [7] 1161-67 (2004).
12. Y. Saito, H. Takao, T. Tani, T. Nonoyama, K. Takatori, T. Homma, T. Nagaya, and M. Nakamura, "Lead-Free Piezoceramics," *Nature*, **432** 84-7 (2004).
13. A. J. Jacobson and B. E. F. Fender, "A Neutron Diffraction Study of the Nuclear and Magnetic Structure of BiFeO_3 ," *J. Phys.*, **C8** [6] 844-50 (1975).
14. T. Kimura and T. Yamaguchi, "Fused Salt Synthesis of $\text{Bi}_4\text{Ti}_3\text{O}_{12}$," *Ceram. International*, **9** [1] 13-7 (1983).
15. F. K. Lotgering, "Topotactical Reactions with Ferrimagnetic Oxides Having Hexagonal Crystal Structures-I," *J. Inorg. Nucl. Chem.*, **9** [2] 113-23 (1959).
16. Y. Seno and T. Tani, "TEM Observation of a Reactive Template for Textured $\text{Bi}_{0.5}(\text{Na}_{0.87}\text{K}_{0.13})_{0.5}\text{TiO}_3$ Polycrystals," *Ferroelectrics*, **224** [1-4] 793-800 (1999).
17. R. D. Shannon, "Revised Effective Ionic Radii and Systematic Studies of Interatomic Distances in Halides and Chalcogenides," *Acta Crystallogr.*, **A32** [5] 751-67 (1976).
18. K. Fuse and T. Kimura, "Effect of Particle Sizes of Stating Materials on Microstructure Development in Textured $\text{Bi}_{0.5}(\text{Na}_{0.5}\text{K}_{0.5})\text{TiO}_3$," *J. Am. Ceram. Soc.*, **89** [6] 1957-64 (2006).